**Applied Journal of Physical Science**
Volume 7(2), pages 34-48, April 2026
Article Number: 3075AD691
ISSN: 2756-6684
https://doi.org/10.31248/AJPS2026.138
https://integrityresjournals.org/journal/AJPS
*Full Length Research*

# A neural network-based model for addressing global solar radiation data scarcity in tropical and equatorial regions

**Olubusade, J. E.[1,2]*, Oyedum, O. D.[2], Aibinu, M. A.[3], Ezenwora, J. A.[2], Eichie J. O.[2], and Folorunso T. A.[4]**

[1]Department of Mathematical Sciences, Summit University, Offa, Nigeria.
[2]Department of Physics, Federal University of Technology, Minna, Nigeria.
[3]Department of Mechatronics Engineering, Summit University, Offa, Nigeria.
[4]Department of Mechatronics Engineering, Federal University of Technology, Minna, Nigeria.

*Corresponding author. Email: olubusadejoseph@gmail.com



Received Date: 13 March 2026 | Accepted Date: 14 April 2026 | Published Date: 30 April 2026

**ABSTRACT:** Energy is as vital as life itself. Among various energy forms, solar is chief, and its potential to sustain life and other activities on Earth is significant. To achieve optimal efficiency in the design, sizing, calibration, manufacture, or deployment of any solar application, it is crucial to accurately measure the Global Solar Radiation (GSR) at the surface. GSR can be quantified through direct and indirect methods. Data obtained via the direct method is considered more accurate but scarce. Conversely, data acquired through indirect methods is accessible for any location of interest, but its precision is often doubtful. This study aims to develop a GSR model to address data scarcity, mitigate instances of erroneous estimations, and the intricacy of existing models that attempt to predict GSR. A multi-layer neural network, consisting of 49 neurons in the hidden layer, was selected from multiple training trials from which a new Soft Computing Model (SCM) emerged. The network was trained, tested, and validated using a 25-year dataset on monthly averages, comprising solar flux, relative humidity, and temperature change as the input nodes. A regression coefficient of 0.9832 was obtained during the neural network training phase, indicating a strong agreement between predicted and measured values. To assess the predictive performance of the trained network, a new dataset was introduced for testing, yielding a regression coefficient of 0.9737, a mean squared error of 0.0015 and a mean absolute error of 0.0210 when compared with measured data, representing the best performance among all training iterations. Comparative evaluation with existing models and deployment across different locations confirmed that the SCM consistently performed well. The deployment results further confirmed that the model is well-optimised for tropical and equatorial climates, while recalibration would be required to ensure reliable performance in temperate and high-latitude regions.

**Keywords:** Artificial Neural Network, global solar radiation, renewable energy, solar energy, soft computing model, data scarcity.

## INTRODUCTION

Energy is as fundamental as life itself, and without it, no processes would occur (Besharat *et al*., 2013; Kren *et al*., 2017). Energy is not a tangible entity that can be seen, heard, touched, or smelled. It is not composed of any substance but rather represents a property of matter (Channell and Smith, 2000). Both biotic and abiotic entities necessitate energy, yet the form, state, mode of existence, and utilisation of energy are dynamic. It is crucial to recognise that not all forms of energy can be optimally harnessed; some are non-reusable, while others are reusable. Consequently, it is prudent to explore the most abundant, adaptable, and prevalent source of reusable energy, namely solar energy (Fashina *et al*., 2018; Guler and Bilgin, 2026).

Solar energy is derived from the sun, a massive luminous body of glowing gas (García *et al*., 2007). The sun is an average star and the largest member of the solar system (Temmer, 2021). It sustains life on Earth by facilitating plant growth, nourishing animals, preserving food, heating and illuminating the land, sea, and atmosphere. Additionally, it generates winds and tides, circulates water, and, importantly, produces fossil fuels (Firebaugh *et al*., 1997). Scientific evidence suggests that the sun has existed for approximately $5 \times 10^9$ years and is expected to persist for another $5 \times 10^9$ years (Bonanno *et al*., 2008). Heat and light are the two primary energy resources obtained from the sun, which are converted into various other forms. There are three principal methods for capturing solar energy: photosynthesis, photovoltaic systems, and solar thermal systems. Through photosynthesis, solar energy is stored in green plants as chemical energy. In photovoltaic applications, photons from the sun are absorbed by solar cells to generate electrical energy. Solar thermal systems utilise the sun's heat to drive desirable processes.

Solar energy resources hold substantial significance across various domains, including agriculture, atmospheric science, meteorology, forestry, engineering, and earth and environmental science, among others (Olomiyesan and Oyedum, 2016). The benefits of solar energy are extensive, encompassing the prediction of plant growth and productivity, electricity generation, drying of agricultural produce, seawater desalination, cooking, initiation of chemical processes, weather activity regulation, production of distilled and warm water, and the operation of engines and pumps, as well as heating and cooling technologies (Chegaar and Chibani, 2000; Torshizi and Mighani, 2017). To effectively harness solar energy for optimal use and satisfaction, it is essential to possess precise knowledge of the obtainable solar radiation (insolation) that reaches the surface at the point of application, which is known as the Global Solar Radiation (GSR).

The global scarcity of ground-measured GSR data is primarily attributable to the limited and uneven distribution of meteorological stations equipped with measuring equipment such as pyranometers (Ben Jemaa *et al*., 2013). Although several empirical and theoretical models have been developed to predict GSR and improve data accessibility, but their predictive reliability often remains questionable (Ben Jemaa *et al*., 2013). In response, there is a pressing need for the development of robust and dependable models for estimating GSR, which is essential for supporting the attainment of Sustainable Development Goal 7 (SDG 7) and other targets related to clean, affordable, and sustainable energy. To address this gap, the study aims to mitigate the challenge of GSR data scarcity by developing a novel artificial neural network-based GSR model.

## REVIEW OF LITERATURE

The potential of the Sun to sustain life and support numerous activities on Earth cannot be underestimated (Besharat *et al*., 2013). Solar energy remains the most available, applicable, and abundant energy resource on Earth. Nevertheless, excessive solar heating can sometimes lead to undesirable heat stress and elevated environmental temperatures. Consequently, extensive research efforts are ongoing worldwide, both to harness substantial energy from the Sun and to mitigate its adverse environmental impacts. For effective exploration and utilisation of solar energy, a clear understanding of key terms commonly used in radiation studies is essential.

*Extra-terrestrial radiation* refers to the measurable solar radiation at the outer boundary of the Earth's atmosphere, and it is not influenced by atmospheric processes. The maximum radiation obtainable at this surface is referred to as the solar constant, and it varies with the time of day and months of the year (Skakun and Volobuev, 2017). The solar constant ranges between 1353 and 1394 $Wm^{-2}$; however, for the sake of uniformity, an average value of 1367 $Wm^{-2}$ is widely accepted (Li *et al*., 2011; Abbot and Fowle, 1911). Deviations of extra-terrestrial radiation from the solar constant have been attributed to solar activities such as sunspots and solar bursts, which alter the intensity of energy released by the Sun, as well as the elliptical orbit of the Earth around the Sun (Abbot and Fowle, 1911). The latter can be accounted for using the solar flux relationship given by Kreith and Kreider (2000):

$$I_{rr} = I_{sc}\left[1 + 0.033\ cos\left(\frac{72dn}{73}\right)\right] \quad (1)$$

Where dn is the day number of the year, $I_{sc}$ is the solar constant = 1,367 $Wm^{-2}$ and $I_{rr}$ is the intermittent variation of the extra-terrestrial solar radiation (solar Flux).

*Direct radiation* describes the portion of solar radiation that reaches the Earth's surface without being scattered, and it is usually considered to be perpendicular to the Sun's rays (Piedallu and Gegout, 2007). In contrast, *diffuse radiation* refers to the component of solar radiation that has been scattered or reflected by atmospheric constituents before reaching the Earth's surface (Wald, 2019). *Global Solar Radiation* (GSR) encompasses both direct and diffuse components, representing the total measurable solar radiation on the Earth's surface. As such, GSR is the factor of primary importance in solar applications. However, the magnitude of GSR received per unit surface area varies geographically, as well as with time and season. Factors influencing GSR variation include, but are not limited to, solar flux, solar inclination angle, cloud amount, relative humidity, atmospheric thickness, time of day, day number of the year, latitude,and altitude (Skakun and Volobuev, 2017).

## Measurement and modelling of GSR

Global Solar Radiation can be obtained through either direct measurement or indirect estimation methods. Direct measurement involves the installation of instruments such as pyranometers for real-time logging of GSR data. This approach is generally associated with high precision and accuracy. However, its widespread application is limited by several challenges, including high capital costs, scarce skilled technical personnel, inadequate maintenance budgets, and demanding operational requirements. These limitations explain the scarcity of GSR data globally, as many meteorological stations cannot afford the essential requirements (Gueymard and Myers, 2009). In contrast, the indirect method involves the estimation of GSR using mathematical or empirical models. This approach attempts to bridge the wide gap between GSR data scarcity and availability. In order to improve GSR data availability, researchers have developed mathematical models for estimating GSR across different locations. Though the credibility and accuracy of model predictions are often not satisfactory (Wallace and Hobbs, 2006; Ertekin, 2007; Fan *et al*., 2019).

GSR modelling parameters can be grouped into physical parameters (albedo, atmospheric transmittance, aerosol optical depth, ozone column, cloud column, and atmospheric scattering particles), astronomical parameters (Sun-Earth distance, solar constant, extra-terrestrial radiation, solar declination angle, and solar hour angle), geographical parameters (longitude, latitude, and altitude), and geometrical parameters (tilt angle, surface azimuth, solar altitude, and solar azimuth) (Menges *et al*., 2006; Besharat *et al*., 2013).

Most prevailing GSR models are empirical models, which are widely used due to their simplicity and reliance on commonly available meteorological parameters. Empirical models often correlate regression coefficients and atmospheric parameters with the clearness index (Teke *et al*., 2015). In contrast, some models rely heavily on physical parameters and are therefore referred to as physical models (Dazhia *et al*., 2012). It is also noteworthy that while some models adopt a single parameter approach for GSR estimation, others incorporate multiple parameters. This distinction is therefore used as a basis for the classification of existing models in the next subsections.

### *Temperature-based empirical model*

Temperature-based models employ minimum and maximum air temperature in correlation with the clearness index to estimate global solar radiation. Models in this category are developed on the basis of atmospheric transmissivity. Examples include the works of Hargreaves and Samani (1982), Bristow and Campbell (1984), Allen (1997), Goodin (1999), Thornton and Running (1999), Meza and Veras (2000), Weiss *et al.* (2001), Winslow (2001), Annandale *et al*. (2002), Chen *et al*. (2004), Falayi (2008), Li *et al.* (2010), Adaramola (2012), Ohunakin *et al*. (2013), Jahani *et al.* (2017) and Fan *et al.* (2018).

### *Cloud-based empirical models*

GSR is largely modulated by cloud (Muneer and Gul, 2000; Sanchez *et al*., 2012). Among the factors that are responsible for solar radiation balance on the surface of the Earth, clouds display huge uncertainty in their characterisation and quantification (Norris, 1968). The works of Black (1956), Lumb (1964), Paltridge (1976), Daneshyar (1978), Kasten and Czeplak (1980), and Badescu (1999) are common examples.

### *Sunshine-based empirical models*

This category of GSR models presumes that the intensity and the duration of sunshine are good predictors of GSR. This is achieved by correlating the fraction of the available sunshine hours and the possible hours of sunshine (day length) with the clearness index. The works of Angstrom-Prescott (1924), Prescott (1940), Glover and McCulloch (1958), Page (1961), Rietveld (1978), Dogniaux and Lemoine (1983), Kilic and Ozturk (1983), Ögelman *et al.* (1984), Zabara (1986), Bahel (1987), Gopinathan (1988), Newland (1989), Luhanga and Andringa (1990), Raja (1994), Elagib and Mansell (2000), Almorox and Hontoria (2004), El-Metwally (2005), Jin *et al*. (2005), Rensheng *et al*. (2006), Bakirci (2009), Gana and Akpootu (2013), Teke and Yildirim (2014) are good examples (Yelmen *et al.,* 2022).

### *Multiple parameter-based empirical models*

The multiple parameter-based models are often referred to as hybrid parameter-based models (Olomiyesan and Oyedum, 2016). The model combines two or more parameters to predict GSR. Some of the commonly combined parameters include air temperature, sunshine duration, relative humidity, cloud cover, amount of rainfall, atmospheric pressure, soil temperature and dew point temperature. Unlike the single parameter-based models, multiple parameter-based models are developed on the basis that the balance of solar radiation is determined by many factors in the atmosphere, and they are deemed to be more reliable in their prediction accuracy (Quej *et al*., 2016). Prominent examples are seen in the works of Swartman and Ogunlade (1967), Sabbagh (1977), Gariepy (1980), Garg and Garg (1982), Ojosu and Komolafe (1987), Abdalla (1994), Ododo *et al.* (1995),

Allen (1995), Hunt *et al*. (1998), Akpabio *et al*. (2004), Chandel *et al*. (2005), Chen *et al*. (2006), Wu *et al*. (2007), Maghrabi (2009), Olayinka (2011), Antonanzas *et al.* (2013), Ouali and Alkama (2014), Okundamiya *et al. (*2015), and Olomiyesan and Oyedum (2016). Aside from the empirical models, another indirect means for predicting GSR is by soft computing (Xue and Zhou, 2019).

### *Soft computing method*

Soft computing is predicated on the basis of computer Artificial Intelligence (AI). It has been identified as the best predictor when comparing complex situations (Maqsood *et al*., 2004). The method includes Artificial Neural Network (ANN), Recurrent Neural Network, Support Vector Machine, Genetic Algorithm, Radial Basis Function Network and Artificial Neuro-Fuzzy Inference System, to mention a few (Mohanty *et al*., 2016; Xue and Zhou, 2019). ANN, which imitates the method of information processing of the human brain, is the most prominent among the soft computing models (Fadare *et al*., 2010). ANN is a set of processing units that is represented by artificial neurons, which are connected by artificial synapses to perform parallel distributed processes that are controlled by vectors and matrices of synaptic weights (Shepherd, 2004; Eichie *et al.,* 2016; Folorunso *et al*., 2019; da Silva *et al*., 2016). The works of the following researchers are good examples: Gardner and Dorling (1998), Hsieh and Tang (1998), Maqsood *et al*. (2002), Fadare *et al*. (2010), Kumar *et al*. (2012), Yadav and Chandel (2013), Mantzari and Mantzaris (2013), Mohanty *et al.* (2016), Quej *et al.* (2017), Kamadinata *et al.* (2017), Mohamed (2019), Fan *et al.* (2019), Aljanad *et al.* (2021), Huang *et al*. (2022), Apeh and Nwulu (2024), Xu *et al*. (2025), Guler and Bilgin (2026), and Fohagui *et al*. (2026).

### Research gap

In general, empirical models have integrated extra-terrestrial solar radiation ($H_o$) in their frameworks. $H_o$ is represented in a simplified form in Equation (2a) and in its expanded form in Equation (2e):

$$H_o = \frac{24}{\pi} I_{sc}\left[1 + 0.033\cos\frac{360dn}{365}\right] \times \left[cos\varphi.cos\delta.sin\omega_s + \frac{\pi}{180}\omega_s.sin\varphi.sin\delta\right] \quad (2a)$$

Given that;

$$\delta = 23.45\ \sin\left[\frac{360\ (284+dn)}{365}\right] \quad (2b)$$

$$\omega_s = cos^{-1}(-tan\varphi.tan\delta) \quad (2c)$$

$$s_o = \frac{2}{15}\omega_s \quad (2d)$$

Substituting for $\delta$, $\omega_s$ and $s_o$ in Equation (2a) gives:

$$H_o = \frac{24}{\pi} I_{sc}\left[1 + 0.033\cos\frac{360dn}{365}\right][cos\varphi]\left[cos\left(23.45\sin\left(\frac{360\ (284+dn)}{365}\right)\right)\right] \times \left[\sin\langle cos^{-1}\left\{[-tan\varphi]\left[tan\left(23.45\sin\left(\frac{360\ (284+dn)}{365}\right)\right)\right]\right\}\rangle\right] + \frac{\pi}{180}\left[cos^{-1}\left\{[-tan\varphi]\left[tan\left(23.45\sin\left(\frac{360\ (284+dn)}{365}\right)\right)\right]\right\}\right][sin\varphi]\left[sin\left(23.45\sin\left(\frac{360\ (284+dn)}{365}\right)\right)\right] \quad (2e)$$

Where: $\omega_s$ is the sunset hour angle; $\varphi$ is the latitude of the site; $\delta$ is the solar declination; and $s_o$ is the average day length.

However, this approach is not particularly user-friendly due to the complex mathematical calculations required to determine the values of $H_o$, which can lead to significant computational errors.

It is also good to note that some existing GSR estimation models remain limited by their inability to effectively represent complex atmospheric non-linearity, thereby resulting in inconsistent accuracy and dependence on assumptions (Dickinson, 2003; Shen *et al*., 2022; Huang *et al*., 2022). Again, many of the existing models lack innovation due to heavy reliance on modifications and amalgamation of earlier approaches, while some other models suffer from poor transferability across locations. In addition, high computational demands and the need for scarce input parameters have reduced the practicality of certain GSR models (Antonanzas *et al*., 2013; Bojanowski *et al*., 2013). Conversely, existing soft computing models have not adequately addressed this issue, as they are also presented in complex formats requiring a certain level of expertise (Apeh and Nwulu, 2024; Xu *et al*., 2025; Fohagui *et al*., 2026; Guler and Bilgin, 2026). Hence, the proposed model aims to address GSR data scarcity through a user-friendly approach to mitigate erroneous estimations and the intricacy of existing models that attempt to predict GSR (Veeraboina and Guduri, 2014).

Figure 1 describes the fundamental structure of a neural network. The output y of the network is given as:

$$y = \sum_{i=1}^{n}(w_i\, x_i\ + \ldots\ldots + w_n\, x_n) \quad (3)$$

$$y = (w^T x) \quad (4)$$

Where:

$$w^T = (w_1,\ w_2, w_3, \ldots\ldots w_n)^T \quad (5)$$

$$x = (x_1,\ x_2, x, \ldots\ldots x_n) \quad (6)$$

By introducing a bias value and activation function, the equation becomes:

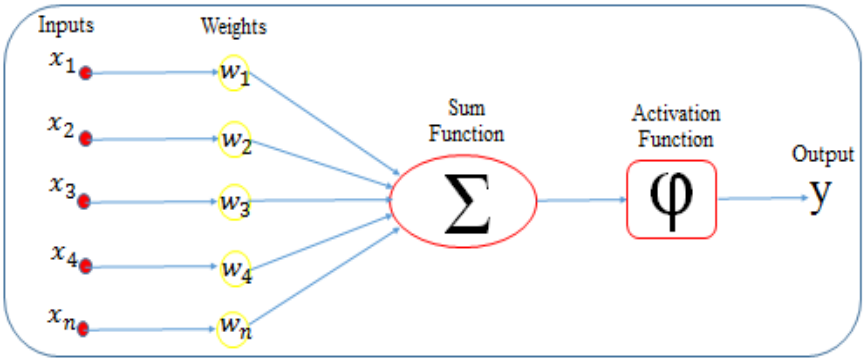


**Figure 1.** Artificial neuron.

$$y = \varphi\left(\sum_{i=1}^{n}(w_i x_i + \ldots\ldots + w_n x_n + b_1)\right) \quad (7)$$

$$y = \varphi\left(\sum_{i=1}^{n}(w^T x + b_1)\right) \quad (8)$$

For a network of two output layers, then the equation becomes:

$$y_2 = \gamma\left[\sum_{i=1}^{n}\left(w_j y + b_2\right)\right] \quad (9)$$

$$y_2 = \gamma\left[\sum_{i=1}^{n}\left(w_j \varphi\left\langle\sum_{j=1}^{m}((w_i x_i + \ldots\ldots + w_n x_n + b_1)\right\rangle + b_2\right)\right] \quad (10)$$

$$y_2 = \gamma\left[\sum_{i=1}^{n}\left(w_j \varphi\left\langle\sum_{j=1}^{m}(w^T x + b_1)\right\rangle + b_2\right)\right] \quad (11)$$

Where *w* is the weight of the respective variables, $w^T$ is the transpose of the weight, $b_1$ and $b_2$ are biases, φ and γ are the activation functions, $x$ is the input variable, while *y* and $y_2$ are the outputs of the network, i, j, n and m are positive integers.

## METHODOLOGY

Figure 2 describes the major process involved in training an ANN for model development, while Figure 3 shows the setup of the Photovoltaic Research Station in Federal University of Technology, Minna, Nigeria. Materials used for the study include: Li-200SA Pyranometer, solar panel, laptop computer, data logger, MATLAB, and meteorological/atmospheric dataset.

A 25-year (1993 to 2018) dataset comprising monthly averages of global solar radiation, relative humidity, cloud cover, rainfall, minimum temperature, and maximum temperature was sourced from the National Aeronautics and Space Agency (NASA) database for multiple locations in North Central Nigeria (https://power.larc.nasa.gov/data-access-viewer/). North Central Nigeria is climatically diverse. It is located in a transition zone between the humid south and arid north. The climatic variation also supports both the Guinea and the Sudan savanna. To validate the satellite data, ground measurements were taken using a Li-200SA Pyranometer between December 2015 and November 2018. A mean percentage error of 8% and a mean square error of 0.30 were recorded as the error margin.

Multiple datasets from various point locations in North Central Nigeria were employed to train a multilayer perceptron ANN, leading to the development of a Soft Computing Model (SCM) that demonstrated optimal performance when deployed across multiple sites. Furthermore, a 10-year dataset (2015–2024) comprising monthly averages of global solar radiation, relative humidity, and minimum and maximum temperatures was sourced from NASA (www.power.larc.nasa.gov/data-access-viewer/) for different countries listed in Table 1, to further validate the SCM. Model performance was evaluated using standard statistical metrics, including Mean Absolute Error, Mean Bias Error, Mean Percentage Error and Root Mean Squared Error.

### Data instrument and data pre-processing

The Li-200SA Pyranometer is engineered to measure GSR at a five-minute integration time in field conditions characterised by clear and unobstructed daylight, as depicted in Figure 3. It employs a silicon photovoltaic sensor with a maximum error margin of approximately ±5% under natural daylight conditions. The sensitivity of the LI-200SA is fundamentally 90μA per 1000W, with a response time of 10μs, and a temperature tolerance ranging from -40 to 65°C, which is comparable to the globally recognised thermopile-type Pyranometer (Nwokolo and Ogbulezie, 2018; Olubusade *et al*., 2022).

Filtering of the datasets was done in order to get rid of invalid data, while missing data was replaced by the average of neighbouring (preceding and succeeding) data. In addition, the ground-measured datasets were converted into monthly averages, corresponding to the sourced satellite datasets.

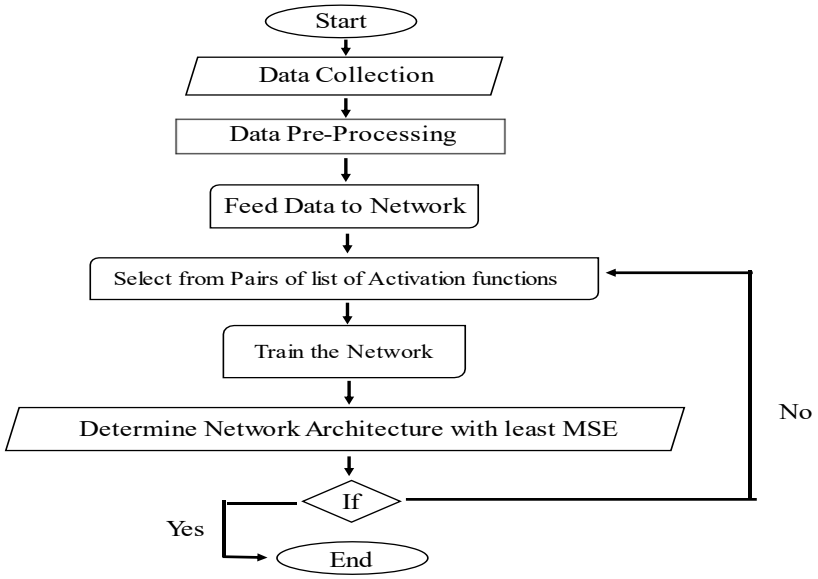


**Figure 2.** Flowchart of the ANN training.

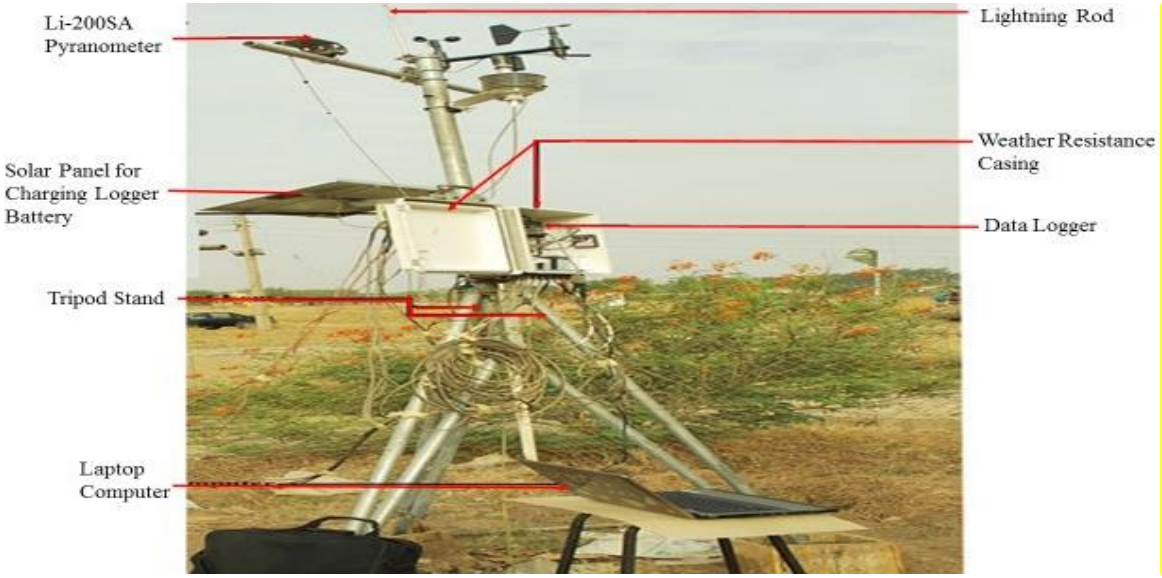


**Figure 3.** Photovoltaic Research Station, Federal University of Technology, Minna.

## ANN design

The design considered a varying combination of parameters, including relative humidity, cloud cover, rainfall, minimum temperature, sunshine hours, maximum temperature and temperature range as inputs to the network. A combination of Relative Humidity (RH), Temperature range ($T_{max} - T_{min}$) and solar flux ($I_{rr} = I_{sc}\left[1 + 0.033cos\langle\frac{dn*72}{73}\rangle\right]$) is most desirable for use after deployed to estimate GSR for different locations. They are therefore documented as the three inputs to the ANN network as shown in Figure 4, where $I_{sc}$ is solar constant and dn is the day number of the year. After a validity check on the acquired datasets, it was normalised to ensure even distribution (Folorunso *et al*., 2019). Normalising the dataset is achieved using the 'minmax' approach. This is done to ensure data conformity with the transfer functions. Measured GSR is the target of the network, while the network-predicted GSR is the output. The proposed SCM is developed using a multi-layer neural network consisting of three nodes at the I nput layer, varying neurons at the

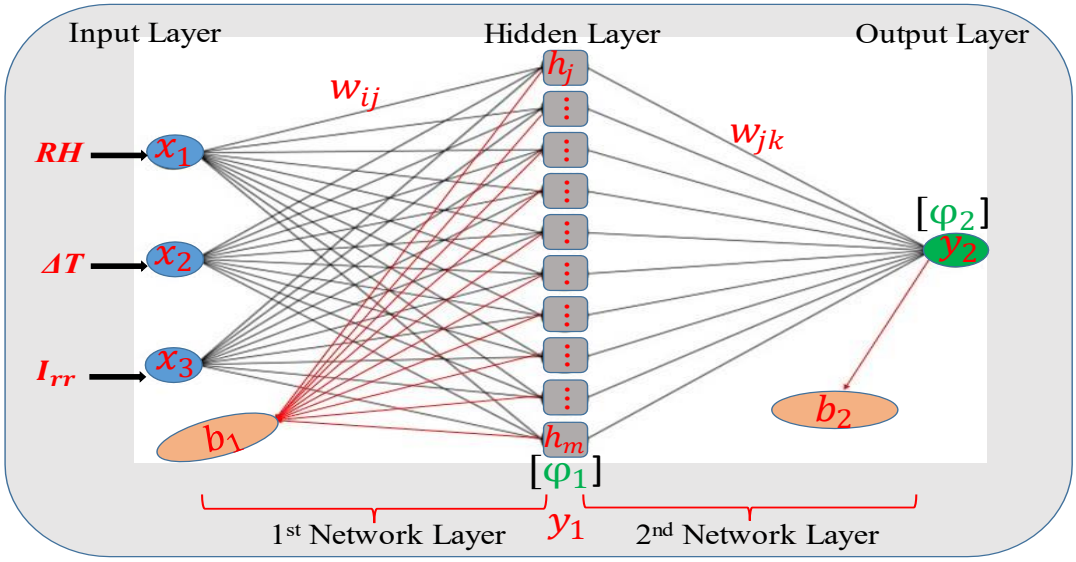


**Figure 4.** Multi-Layer Neural Network.

hidden layer, and one node at the output layer. The network training process employed the feedforward back-propagation network (Shahin *et al*., 2008; al Shamisi *et al*., 2011; Nguyen *et al*., 2019), and it is a supervised learning process that adopts the Levenberg-Marquard training algorithm (TRAINLM). MATLAB was used to write the script files for the developed SCM. The script files were written to assess and determine the relative effect of weights, biases, number of neurons in the hidden layer, and the accurate combination of the activation functions to obtain the best ANN's performance. Furthermore, a varying number of neurons in the hidden layer was considered from 2 to 100 in line with Heuristic principles for the design of ANN (Walczak and Cerpa, 1999). Non-linear activation functions ($\varphi_1$) which include Logsig and tansig (Karlik and Olgac, 2011; Han and Moraga, 1995). were variably used at the first layer of the network, while purelin, a linear activation function ($\varphi_2$) was used at the second layer of the network (Eichie *et al*., 2016) $\varphi_2$ is assumed at the second layer of the network, such that a linear model can be established, while $\varphi_1$ is used at the first layer of the network, such that different solutions can be obtained from the complex relationships between parameters.

The mathematical representation of Figure 4 is given by:

$$y_2 = \varphi_2\left[\sum_j^m\left(w_{jk}\langle\varphi_1\left(\sum_i^n\left(w_{ij}x_i + b_j\right)\right)\rangle + b_k\right)\right] \quad (12)$$

where all parameters have retained their initial properties and identities.

**Derivation of the model equation**

The model is obtained from Figure 4 and Equation 12.

$$y_1 = \varphi_1\,(IW \cdot x + b_1) \quad (13)$$

$$y_2 = \varphi_2[LW\,(y_1) + b_2] \quad (14)$$

$$y_2 = \varphi_2[LW\,(IW \cdot x\varphi_1 + b_1\varphi_1) + b_2] \quad (15)$$

For which $\varphi_1$ is a non-linear activation function then, $f(x) \neq x$ and $\varphi_2$ is a linear activation function, such that $f(x) = x = 1$.

$$y_2 = [(LW \cdot IW \cdot x)\varphi_1 + (LW \cdot b_1)\varphi_1 + b_2] \quad (16)$$

where IW is a [m × 3] matrix, LW is a [1 × m] matrix, $b_1$ is a [m × 3] matrix

let $LW \cdot IW$ = [t, u, v] matrix (17)

$$x = \begin{bmatrix} O \\ P \\ Q \end{bmatrix} \quad (18)$$

$$(LW \cdot IW \cdot x)\varphi_1 = [t, u, v]\begin{bmatrix} O \\ P \\ Q \end{bmatrix} \quad (19)$$

$$(LW \cdot IW \cdot x)\varphi_1 = \text{tO + uP + vQ} \quad (20)$$

$$(LW \cdot b_1)\varphi_1 = [z] \quad (21)$$

$$\boldsymbol{y_2} = \text{tO + uP + vQ + z + } b_2 \quad (22)$$

$$\alpha = z + b_2 \quad (23)$$

$$\boldsymbol{y_2} = \text{tO + uP + vQ + } \alpha \quad (24)$$

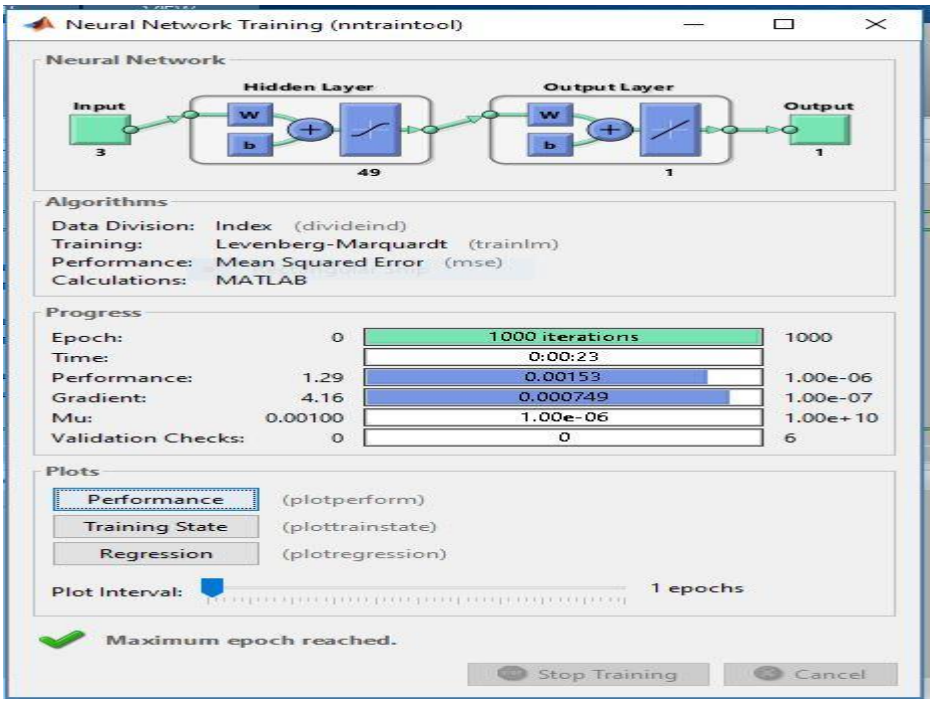


**Figure 5.** Neural network training tool.

Hence, the developed model takes the form:

$$H = t(RH) + u(\Delta T) + v(I_{rr}) + \alpha \quad (25)$$

where $\varphi_1$ and $\varphi_2$ are activation functions of the first and second layers respectively, $b_j = b_1$ is the input bias that is associated with the j[th] neuron of the first layer, $b_k = b_2$ is the output bias that is associated with the k[th] neuron of the second layer, $w_{ij}$ is the adjustable weight that connects the input layer to the hidden layer, $w_{jk}$ is the adjustable weight that connects the hidden layer to the output layer, (for which $1 \leq j \leq m$, that is, the total number of neurons in the hidden layer), $x_i$ is the set of input data to the ANN (for which $1 \leq i \leq n$ and n = 3), $y_1$ is the output of the first layer while $y_2$ is the output of the second layer, z is a derivative of the product of the layered weights and the input biases, it is a 1 by 1 matrix, t, u, v = are constants derived from the product of the layered and input weights, O, P, Q = are input vectors which represent relative humidity (RH), temperature change ($\Delta T$) and solar flux ($I_{rr}$) respectively, also, LW ≡ $w_{jk}$ while, IW ≡ $w_{ij}$.

**Training and testing the state of the ANN**

The dataset used in the process consists of 300 samples (that is, monthly average datasets from January to December for 25 years), with 210 samples (70%) allocated for training, 45 samples (15%) for testing, and the remaining 45 samples (15%) for validation. A multi-layer neural network was trained as depicted in the nntrainingtool in Figure 5. The optimal network configuration from multiple training trials comprises 49 neurons in the hidden layer, utilising tansig and purelin as the selected activation function pair for the first and second layer of the network, respectively, in which a regression coefficient of 0.9832 was achieved for the training phase, and 0.9737 for the testing phase, representing the best possible performance across all training trials. The Mean Squared Error (MSE) was recorded at 0.0015, and the Mean Absolute Error (MAE) at 0.0210. In addition, the damping factor (Mu) is 0.0000001, which is low compared to the maximum allowable limit, reflecting stable and faster convergence behaviour.

In accordance with the above results, the values of the constants are given as:

t = 0.0181, u = 0.1486, v = 0.0015, z = 0.3876, $b_2$ = -0.7606, α = -0.373

where H is the GSR, RH is the relative humidity, $\Delta T$ is the change in temperature, $I_{rr}$ is the solar flux, t, u, v, z, $b_2$ and α are constants as expressed in equation (25).

**Performance assessment of SCM**

GSR was estimated using the SCM alongside thirteen other existing empirical models for comparative performance

**Table 1.** Name and description of locations.

| Sn | Location | Latitude (º) | Longitude (º) |
|---|---|---|---|
| 1 | Australia | -26.44 | 133.28 |
| 2 | Brazil | -15.79 | -47.88 |
| 3 | Cameroon | 3.84 | 11.50 |
| 4 | Canada | 55.36 | -100.44 |
| 5 | China | 34.05 | 102.41 |
| 6 | Colombia | 3.05 | -73.49 |
| 7 | Egypt | 30.03 | 31.23 |
| 8 | Ghana | 5.61 | -0.21 |
| 9 | India | 20.59 | 78.96 |
| 10 | Malaysia | 3.80 | 101.69 |
| 11 | Nigeria | 9.22 | 7.85 |
| 12 | South Africa | -28.48 | 24.67 |
| 13 | Togo | 8.62 | 0.82 |

ce analysis using statistical metrics. The empirical models employed include both single-parameter and multiple-parameter models. The single-parameter models comprise the Hargreaves and Samani Model (Md 1), Bristow and Campbell Model (Md 2), Annadale Model (Md 3), Allen Model (Md 4), Angstrom-Prescott Model (Md 5), Glover and McCulloch Model (Md 6), Ogleman Model (Md 7), and Newland Model (Md 8). The multiple-parameter models include the Swartman and Ogunlade Model (Md 9), Abdalla Model (Md 10), Okundamiya Model (Md 11), Olomiyesan and Oyedum Model (Md 12), and Badescu Model (Md 13). To further evaluate the applicability of the developed SCM beyond Nigeria, it was implemented in some selected countries. The selected countries and their respective coordinates are presented in Table 1.

## RESULTS AND DISCUSSION

For all combinations of activation functions, an increase in the number of neurons within the hidden layer enhances the network's performance, with a corresponding decrease in the MSE and the MAE. Therefore, an appropriate number of neurons facilitates effective generalisation of results; conversely, an insufficient number of neurons leads to underfitting due to suboptimal training and testing performance, while an excessive number of neurons results in overfitting, characterised by strong training performance but poor generalisation (Walczak and Cerpa, 1999; Ogunbo *et al*., 2020; Sharkawy, 2024; Ni *et al*., 2026). The effect of RH is most significant on GSR. This is owing to the fact that an increase in RH would result in a corresponding increase in atmospheric water vapour and cloud, which absorbs, reflects and scatters solar radiation, thereby reducing the magnitude of GSR at the Earth's surface (Alemu, 2025). On the other hand, the effect of $\Delta T$ on GSR is intermediate. It has an indirect effect on GSR. However, it is good to note that clear skies would result in an increased GSR and a corresponding increase in $\Delta T$. In addition, $I_{rr}$ represents the maximum potential solar energy at the top of the atmosphere and has the least influence on GSR owing to its relatively constant values (Skakun and Volobuev, 2017).

GSR was estimated using fourteen GSR models and compared with measured GSR (MGSR) datasets. Information regarding the performance of the various models in comparison to the MGSR is presented in Figure 6 and Table 2. The graphical illustration in Figure 6 indicates that the values of the SCM closely approximate the MGSR (Maqsood *et al*., 2004; Fohagui *et al*., 2026; Guler and Bilgin, 2026). The accuracy of the SCM is further corroborated by Table 2, which shows lower values that are desirable for MAE, MBE, MSE, and RMSE, and a higher value approaching unity for the R.

When deployed to different point locations, results showed that the SCM performs very well in tropical and equatorial regions such as Nigeria, Malaysia, Colombia, Brazil, Cameroon, Ghana, and Togo with corresponding low error values, indicating strong accuracy and reliability. This suggests that the model is well-tuned to climates similar to Nigeria's, where solar conditions are relatively stable and consistent with the tropics. However, the model's performance deteriorates significantly in mid- and high-latitude regions, with particularly poor results for Canada and China, showing severe underestimation. Furthermore, countries like Australia, Egypt, South Africa, and India also recorded significant errors with consistent underestimation, which is likely due to differences in atmospheric turbidity, seasonality and solar angles compared to Nigeria. Findings, as shown in Figure 7 and Table 3, confirm that the SCM is effective in Africa, South America, and Southeast Asia, but requires significant adjustment before global application. Figure 7 describes the relationship between the measured and the estimated

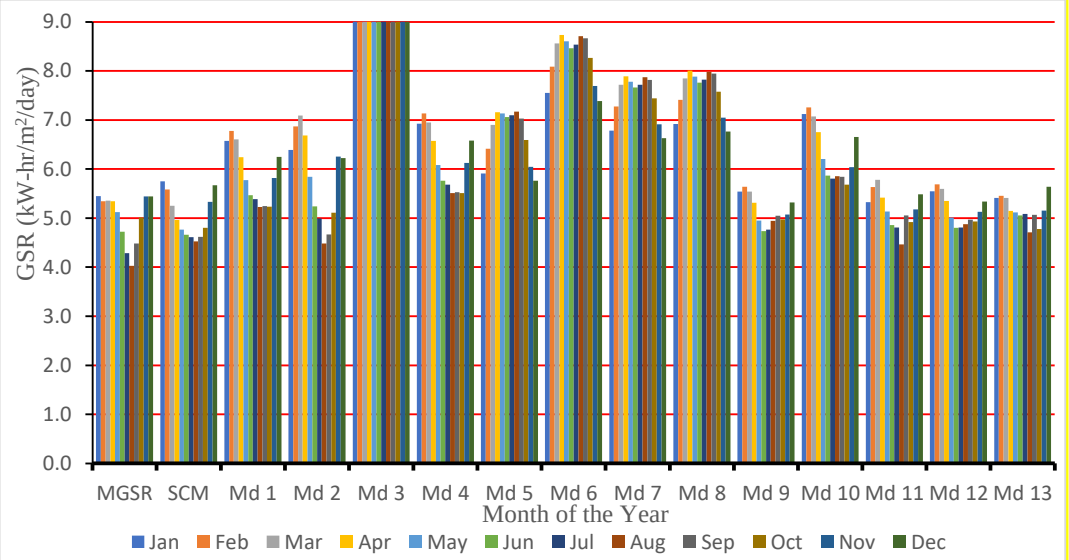


**Figure 6.** Comparison of estimated GSR with measured GSR for different models.

**Table 2.** Evaluation of GSR models.

| Sn | Model | MAE | MBE | MSE | RMSE | R |
|---|---|---|---|---|---|---|
| 1 | Md 1 | 0.881 | -0.881 | 0.896 | 0.947 | 0.789 |
| 2 | Md 2 | 0.819 | -0.819 | 0.904 | 0.951 | 0.887 |
| 3 | Md 3 | 15.266 | -15.266 | 252.096 | 15.878 | 0.817 |
| 4 | Md 4 | 1.195 | -1.195 | 1.558 | 1.248 | 0.788 |
| 5 | Md 5 | 1.688 | -1.688 | 3.650 | 1.910 | -0.645 |
| 6 | Md 6 | 3.270 | -3.270 | 11.401 | 3.377 | -0.603 |
| 7 | Md 7 | 2.456 | -2.456 | 6.705 | 2.589 | -0.611 |
| 8 | Md 8 | 2.579 | -2.579 | 7.308 | 2.703 | -0.604 |
| 9 | Md 9 | 0.273 | -0.153 | 0.142 | 0.377 | 0.702 |
| 10 | Md 10 | 1.344 | -1.344 | 1.972 | 1.404 | 0.707 |
| 11 | Md 11 | 0.249 | -0.170 | 0.098 | 0.313 | 0.842 |
| 12 | Md 12 | 0.269 | -0.168 | 0.129 | 0.359 | 0.760 |
| 13 | Md 13 | 0.294 | -0.167 | 0.150 | 0.388 | 0.705 |
| 14 | SCM | 0.247 | -0.043 | 0.077 | 0.277 | 0.825 |

**Table 3.** SCM performance in different countries.

| Sn | Location | MAE | MBE | MPE (%) | RMSE |
|---|---|---|---|---|---|
| 1 | Australia | 1.26 | -0.26 | 10.73 | 1.43 |
| 2 | Brazil | 0.40 | -0.18 | 3.39 | 0.46 |
| 3 | Cameroon | 0.42 | -0.40 | 9.94 | 0.53 |
| 4 | Canada | 4.49 | -4.49 | 399.36 | 5.17 |
| 5 | China | 2.16 | -2.16 | 55.52 | 2.40 |
| 6 | Colombia | 0.27 | -0.05 | 1.57 | 0.31 |
| 7 | Egypt | 1.52 | -0.43 | 18.03 | 1.72 |
| 8 | Ghana | 0.85 | 0.85 | 16.91 | 0.92 |
| 9 | India | 0.94 | -0.54 | 13.50 | 1.13 |
| 10 | Malaysia | 0.26 | 0.11 | 1.89 | 0.29 |
| 11 | Nigeria | 0.27 | 0.07 | 0.61 | 0.32 |
| 12 | South Africa | 1.38 | -0.73 | 19.59 | 1.61 |
| 13 | Togo | 0.37 | -0.08 | 2.21 | 0.41 |

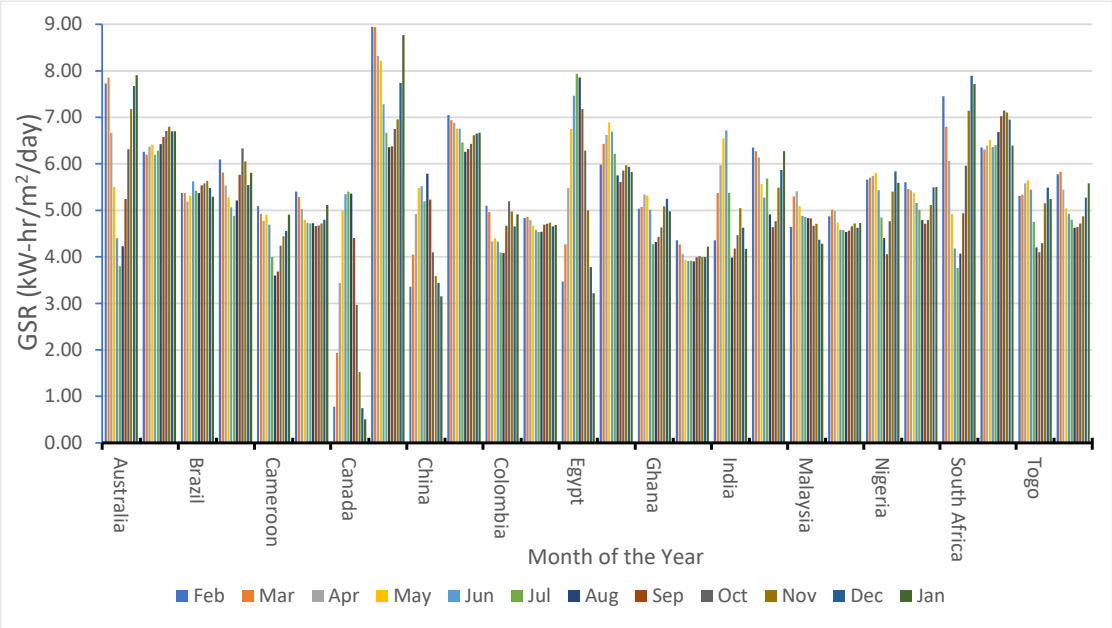


**Figure 7.** Comparison of estimated GSR with measured GSR in different countries.

GSR for each point location under investigation.

## Conclusion and Recommendation

Solar energy plays a crucial role in the anticipated future of energy transition and its vast applicability is irrefutable. A precise knowledge of incoming solar radiation is essential for each point of application and the desired technology. Establishing a comprehensive global database of GSR is crucial for enhancing international solar energy planning, facilitating global marketing, and supporting the design and production of solar-related technologies and services. In response to the persistent challenge of GSR data scarcity, this study has developed an ANN-based SCM to provide reliable estimates of incident solar radiation. SCM was designed to achieve an optimal balance between computational simplicity and predictive accuracy.

From various training ANN trials, a multilayer ANN architecture with 49 neurons in the hidden layer was selected as the most suitable configuration, forming the basis of the proposed SCM, which identifies solar flux, relative humidity, and temperature change as key meteorological parameters that significantly influence the distribution of GSR. During the training phase, the model achieved a regression coefficient of 0.9832, indicating a strong correlation between predicted and measured GSR values. The predictive capability of the trained model was further validated using an independent dataset, which produced a regression coefficient of 0.9737, an MSE of 0.0015, and a MAE of 0.0210, representing the best performance across all training iterations.

To further assess the robustness of the SCM, it was compared with several widely used empirical models, including the Hargreaves and Samani model, Bristow and Campbell model, Annandale model, Allen model, Angstrom–Prescott model, Glover and McCulloch model, Ogleman model, and Newland model. Comparative results demonstrated that the SCM consistently matched or outperformed some of the conventional models in predictive accuracy. Furthermore, the model was deployed and evaluated across multiple geographic locations, including Australia, Brazil, Cameroon, Egypt, Ghana, India, Malaysia, South Africa, and Togo. Findings from these deployments confirmed that the SCM is well-optimised for tropical and equatorial climatic regions. However, results also suggested that recalibration may be necessary to ensure reliable performance of SCM in temperate and high-latitude regions. Hence, the researchers recommended extending the training database by incorporating additional datasets from diverse climatic regions to enhance global scalability and improve the general applicability of the SCM.

## CONFLICT OF INTEREST

The authors declare that they have no conflict of interest.

## REFERENCES

Abbot, C. G., & Fowle, F. E. (1911). The value of the solar constant of radiation. *Astrophysical Journal, 33,* 191p.

Abdalla, Y. A. (1994). New correlations of global solar radiation with meteorological parameters for Bahrain. *International Journal of Solar Energy*, *16*(2), 111-120.

Adaramola, M. S. (2012). Estimating global solar radiation using common meteorological data in Akure, Nigeria. *Renewable Energy*, *47*, 38-44.

Akpabio, L. E., Udo, S. O., & Etuk, S. E. (2004). Empirical correlations of global solar radiation with meteorological data for Onne, Nigeria. *Turkish Journal of Physics*, *28*(3), 205-212.

Al Shamisi, M. H., Ali, H., & Hejase, H. A. (2011). Using MATLAB to develop artificial neural network models for predicting global solar radiation in Al Ain City–UAE. In *Engineering Education and Research Using MATLAB*. https://doi.org/10.5772/25213

Alemu, A. G. (2025). An Investigation of Solar Radiation, Dew Point, Relative Humidity, and Air Temperature in the Afar Region of Ethiopia. *International Journal of Photoenergy*, *2025*(1), 4735627.

Aljanad, A., Tan, N. M., Agelidis, V. G., & Shareef, H. (2021). Neural network approach for global solar irradiance prediction at extremely short-time-intervals using particle swarm optimization algorithm. *Energies*, *14*(4), 1213.

Allen, R. G. (1997). Self-calibrating method for estimating solar radiation from air temperature. *Journal of Hydrologic Engineering*, *2*(2), 56-67.

Almorox, J. Y., & Hontoria, C. J. E. C. (2004). Global solar radiation estimation using sunshine duration in Spain. *Energy Conversion and Management*, *45*(9-10), 1529-1535.

Angstrom, A. (1924). Solar and terrestrial radiation. Report to the international commission for solar research on actinometric investigations of solar and atmospheric radiation. *Quarterly Journal of the Royal Meteorological Society*, *50*(210), 121-126.

Annandale, J., Jovanovic, N., Benade, N., & Allen, R. (2002). Software for missing data error analysis of Penman-Monteith reference evapotranspiration. *Irrigation Science*, *21*(2), 57-67.

Antonanzas-Torres, F., Sanz-Garcia, A., Martínez-de-Pisón, F. J., & Perpiñán-Lamigueiro, O. (2013). Evaluation and improvement of empirical models of global solar irradiation: Case study northern Spain. *Renewable energy*, *60*, 604-614.

Apeh, O. O., & Nwulu, N. I. (2025). Machine learning approach for short-and long-term global solar irradiance prediction. *Journal of Environmental & Earth Sciences*, *7*(1), 321-342.

Badescu, V. (1999). Correlations to estimate monthly mean daily solar global irradiation: application to Romania. *Energy*, *24*(10), 883-893.

Bahel, V., Bakhsh, H., & Srinivasan, R. (1987). A correlation for estimation of global solar radiation. *Energy*, *12*(2), 131-135.

Bakirci, K. (2009). Correlations for estimation of daily global solar radiation with hours of bright sunshine in Turkey. *Energy*, *34*(4), 485-501.

Ben Jemaa, A., Rafa, S., Essounbouli, N., Hamzaoui, A., Hnaien, F., & Yalaoui, F. (2013). Estimation of global solar radiation using three simple methods. *Energy Procedia*, *42*, 406-415.

Besharat, F., Dehghan, A. A., & Faghih, A. R. (2013). Empirical models for estimating global solar radiation: A review and case study. *Renewable and Sustainable Energy Reviews*, *21*, 798-821.

Black, J. N. (1956). The distribution of solar radiation over the earth's surface. *Archiv für Meteorologie, Geophysik und Bioklimatologie, Serie B*, *7*(2), 165-189.

Bojanowski, J. S., Vrieling, A., & Skidmore, A. K. (2013). Calibration of solar radiation models for Europe using Meteosat Second Generation and weather station data. *Agricultural and Forest Meteorology*, *176*, 1-9.

Bonanno, A., Schlattl, H., & Paternò, L. (2002). The age of the Sun and the relativistic corrections in the EOS. *Astronomy & Astrophysics*, *390*(3), 1115-1118.

Bristow, K. L., & Campbell, G. S. (1984). On the relationship between incoming solar radiation and daily maximum and minimum temperature. *Agricultural and Forest Meteorology*, *31*(2), 159-166.

Chandel, S. S., Aggarwal, R. K., & Pandey, A. N. (2005). New correlation to estimate global solar radiation on horizontal surfaces using sunshine hour and temperature data for Indian sites. *Journal of Solar Energy Engineering*, *127*(3), 417-420.

Channell, D. F., & Smith, C. (2000). The science of energy: A cultural history of energy physics in Victorian Britain. *The American Historical Review*, *105*(1), 283-284. https://doi.org/10.2307/2652575

Chegaar, M., & Chibani, A. (2000). A simple method for computing global solar radiation. *Rev. Energ. Ren. Chemss*, 111-115.

Chen, R., Ersi, K., Yang, J., Lu, S., & Zhao, W. (2004). Validation of five global radiation models with measured daily data in China. *Energy Conversion and Management*, *45*(11-12), 1759-1769.

Chen, R., Kang, E., Ji, X., Yang, J., & Zhang, Z. (2006). Trends of the global radiation and sunshine hours in 1961–1998 and their relationships in China. *Energy Conversion and Management*, *47*(18-19), 2859-2866.

Da Silva, I. N., Hernane Spatti, D., Andrade Flauzino, R., Liboni, L. H. B., & dos Reis Alves, S. F. (2016). Artificial neural network architectures and training processes. In *Artificial Neural Networks: A Practical Course* (pp. 21-28). Cham: Springer International Publishing.

Daneshyar, M. (1977). Solar radiation statistics for Iran. *Sol. Energy;(United States)*, *21*(4). https://doi.org/10.1016/0038-092X(78)90013-0.

Dazhi, Y., Jirutitijaroen, P., & Walsh, W. M. (2012). The estimation of clear sky global horizontal irradiance at the equator. *Energy Procedia*, *25*, 141-148.

Dickinson, R. E. (2003). Land-atmosphere interactions. *In: Encyclopedia of Atmospheric Sciences,* Elsevier. Pp. 1116-1120.

Dogniaux, R., & Lemoine, M. (1983). Classification of radiation sites in terms of different indices of atmospheric transparency. In *Solar Radiation Data: Proceedings of the EC Contractors' Meeting held in Brussels, 18–19 October 1982* (pp. 94-107). Dordrecht: Springer Netherlands.

Eichie, J. O., Oyedum, O. D., Ajewole, M. O., & Aibinu, A. M. (2017). Artificial Neural Network model for the determination of GSM Rxlevel from atmospheric parameters. *Engineering Science and Technology, an International Journal*, *20*(2), 795-804.

Elagib, N. A., & Mansell, M. G. (2000). New approaches for estimating global solar radiation across Sudan. *Energy conversion and management*, *41*(5), 419-434.

El-Metwally, M. (2005). Sunshine and global solar radiation estimation at different sites in Egypt. *Journal of Atmospheric and Solar-Terrestrial Physics*, *67*(14), 1331-1342.

Ertekin, C., & Evrendilek, F. (2007). Spatio-temporal modeling of global solar radiation dynamics as a function of sunshine duration for Turkey. *Agricultural and Forest Meteorology*, 145(1-2), 36-47.

Fadare, D. A., Irimisose, I., Oni, A. O., & Falana, A. (2010). Modeling of solar energy potential in Africa using an artificial neural network. *American Journal of Scientific and Industrial Research, 1*(2), 144-157.

Falayi, E. O., Adepitan, J. O., & Rabiu, A. B. (2008). Empirical models for the correlation of global solar radiation with meteorological data for Iseyin, Nigeria. *International Journal of Physical Sciences*, *3*(9), 210-216.

Fan, J., Chen, B., Wu, L., Zhang, F., Lu, X., & Xiang, Y. (2018). Evaluation and development of temperature-based empirical models for estimating daily global solar radiation in humid regions. *Energy*, *144*, 903-914.

Fan, J., Wu, L., Zhang, F., Cai, H., Zeng, W., Wang, X., & Zou, H. (2019). Empirical and machine learning models for predicting daily global solar radiation from sunshine duration: A review and case study in China. *Renewable and Sustainable Energy Reviews*, *100*, 186-212.

Fashina, A. A., Akiyode, O. O., & Sanni, D. M. (2018). The status quo of rural and renewable energy development in Liberia: Policy and Implementation. *SPC Journal of Energy*, *1*(1), 9-20.

Firebaugh, E. B., Behling, S., Behling, S., & Schindler, B. (1997). Sol Power: The Evolution of Solar Architecture by Sophia and Stefan Behling. *Leonardo*, *30*(3), 238-238.

Fohagui, F. C. V., Koholé, Y. W., Ngouleu, C. A. W., Tedom, D. N., & Tchuen, G. (2026). Prediction of Cameroon's global solar radiation using deep learning and machine learning algorithms. *Journal of Atmospheric and Solar-Terrestrial Physics*, 106733.

Folorunso, T. A., Aibinu, M. A., Kolo, J. G., Sadiku, S. O. E., & Orire, A. M. (2019). Water quality index estimation model for aquaculture system using artificial neural network. *Journal of Advances in Computer Engineering and Technology*, *5*(3), 195-204.

Gana, N. N., & Akpootu, D. O. (2013). Angstrom type empirical correlation for estimating global solar radiation in north-eastern Nigeria. *The International Journal Of Engineering And Science*, *2*(11), 58-78.

García, R. A., Turck-Chièze, S., Jiménez-Reyes, S. J., Ballot, J., Pallé, P. L., Eff-Darwich, A., Mathur, S., & Provost, J. (2007). Tracking solar gravity modes: the dynamics of the solar core. *Science*, *316*(5831), 1591-1593.

Gardner, M. W., & Dorling, S. R. (1998). Artificial neural networks (the multilayer perceptron)—a review of applications in the atmospheric sciences. *Atmospheric environment*, *32*(14-15), 2627-2636.

Garg, H. P., & Garg, S. N. (1983). Prediction of global solar radiation from bright sunshine hours and other meteorological data. *Energy Conversion and Management*, *23*(2), 113-118.

Glover, J., & McCulloch, J. S. G. (1958). The empirical relation between solar radiation and hours of sunshine. *Quarterly Journal of the Royal Meteorological Society*, *84*(360), 172-175.

Goodin, D. G., Hutchinson, J. M. S., Vanderlip, R. L., & Knapp, M. C. (1999). Estimating solar irradiance for crop modeling using daily air temperature data. *Agronomy Journal*, *91*(5), 845-851.

Gopinathan, K. K. (1988). A simple method for predicting global solar radiation on a horizontal surface. *Solar & Wind Technology*, *5*(5), 581-583.

Gueymard, C. A., & Myers, D. R. (2009). Evaluation of conventional and high-performance routine solar radiation measurements for improved solar resource, climatological trends, and radiative modeling. *Solar Energy*, *83*(2), 171-185.

Güler, E., & Bilgin, M. Z. (2026). Forecasting Solar Energy Production Using Artificial Neural Networks and Tyrannosaurus Optimization Algorithm. *Sustainability*, *18*(2), 690.

Han, J., & Moraga, C. (1995, June). The influence of the sigmoid function parameters on the speed of backpropagation learning. In *International workshop on artificial neural networks* (pp. 195-201). Berlin, Heidelberg: Springer Berlin Heidelberg.

Hargreaves, G. H., & Samani, Z. A. (1982). Estimating potential evapotranspiration. *Journal of the irrigation and Drainage Division*, *108*(3), 225-230.

Hsieh, W. W., & Tang, B. (1998). Applying neural network models to prediction and data analysis in meteorology and oceanography. *Bulletin of the American Meteorological Society*, *79*(9), 1855-1870.

Huang, H., Band, S. S., Karami, H., Ehteram, M., Chau, K. W., & Zhang, Q. (2022). Solar radiation prediction using improved soft computing models for semi-arid, slightly-arid and humid climates. *Alexandria Engineering Journal*, *61*(12), 10631-10657.

Hunt, L. A., Kuchar, L., & Swanton, C. J. (1998). Estimation of solar radiation for use in crop modelling. *Agricultural and Forest Meteorology*, *91*(3-4), 293-300.

Jahani, B., Dinpashoh, Y., & Nafchi, A. R. (2017). Evaluation and development of empirical models for estimating daily solar radiation. *Renewable and Sustainable Energy Reviews*, *73*, 878-891.

Jin, Z., Yezheng, W., & Gang, Y. (2005). General formula for estimation of monthly average daily global solar radiation in China. *Energy Conversion and Management*, *46*(2), 257-268.

Kamadinata, J. O., Ken, T. L., & Suwa, T. (2017, April). Global solar radiation prediction methodology using artificial neural networks for photovoltaic power generation systems. In *International Conference on Smart Cities and Green ICT Systems* (Vol. 2, pp. 15-22). SCITEPRESS.

Karlik, B., & Olgac, A. V. (2011). Performance analysis of various activation functions in generalized MLP architectures of neural networks. *International journal of artificial intelligence and expert systems*, *1*(4), 111-122.

Kasten, F., & Czeplak, G. (1980). Solar and terrestrial radiation dependent on the amount and type of cloud. *Solar energy*, *24*(2), 177-189.

Kreith, G., & Kreider, J. F. (1978). Principles of solar engineering. *Journal of Solar Energy Engineering*, *122*(2), 114.

Kren, A. C., Pilewskie, P., & Coddington, O. (2017). Where does Earth's atmosphere get its energy? *Journal of Space Weather and Space Climate*, *7*, A10.

Kumar, R., Aggarwal, R. K., & Sharma, J. D. (2015). Comparison of regression and artificial neural network models for estimation of global solar radiations. *Renewable and Sustainable Energy Reviews*, *52*, 1294-1299.

Li, H., Lian, Y., Wang, X., Ma, W., & Zhao, L. (2011). Solar constant values for estimating solar radiation. *Energy*, *36*(3), 1785-1789.

Li, M. F., Liu, H. B., Guo, P. T., & Wu, W. (2010). Estimation of daily solar radiation from routinely observed meteorological data in Chongqing, China. *Energy Conversion and Management*, *51*(12), 2575-2579.

Luhanga, P. V. C., & Andringa, J. (1990). Characteristics of solar radiation at Sebele, Gaborone, Botswana. *Solar Energy*, *44*(2), 77-81.

Lumb, F. E. (1964). The influence of cloud on hourly amounts of

total solar radiation at the sea surface. *Quarterly Journal of the Royal Meteorological Society*, *90*(383), 43-56.
Maghrabi, A. H. (2009). Parameterization of a simple model to estimate monthly global solar radiation based on meteorological variables, and evaluation of existing solar radiation models for Tabouk, Saudi Arabia. *Energy conversion and management*, *50*(11), 2754-2760.
Mantzari, V. H., & Mantzaris, D. H. (2013). Solar radiation: Cloudiness forecasting using a soft computing approach. *Artif. Artificial Intelligence Research*, *2*(1), 69-80.
Maqsood, I., Khan, M. R., & Abraham, A. (2004). An ensemble of neural networks for weather forecasting. *Neural Computing & Applications*, *13*(2), 112-122.
Menges, H. O., Ertekin, C., & Sonmete, M. H. (2006). Evaluation of global solar radiation models for Konya, Turkey. *Energy Conversion and Management*, *47*(18-19), 3149-3173.
Meza, F., & Varas, E. (2000). Estimation of mean monthly solar global radiation as a function of temperature. *Agricultural and Forest Meteorology*, *100*(2-3), 231-241.
Mohamed, Z. E. (2019). Using the artificial neural networks for prediction and validating solar radiation. *Journal of the Egyptian Mathematical Society*, *27*(1), 1-13.
Mohanty, S., Patra, P. K., & Sahoo, S. S. (2016). Prediction and application of solar radiation with soft computing over traditional and conventional approach–A comprehensive review. *Renewable and Sustainable Energy Reviews*, *56*, 778-796.
Muneer, T., & Gul, M. S. (2000). Evaluation of sunshine and cloud cover based models for generating solar radiation data. *Energy Conversion and Management*, *41*(5), 461-482.
Newland, F. J. (1989). A study of solar radiation models for the coastal region of South China. *Solar Energy*, *43*(4), 227-235.
Nguyen, H., Bui, X. N., & Moayedi, H. (2019). A comparison of advanced computational models and experimental techniques in predicting blast-induced ground vibration in open-pit coal mine. *Acta Geophysica*, *67*(4), 1025-1037.
Ni, L., Zhang, S., Huang, K., & Wang, Y. (2026). Multi-level screening method for network security alarms based on DBSCAN algorithm and rete rule inference. *Scientific Reports*, *16*, Article number 5632
Norris, D. J. (1968). Correlation of solar radiation with clouds. *Solar Energy*, *12*(1), 107-112.
Nwokolo, S. C., & Ogbulezie, J. C. (2018). A quantitative review and classification of empirical models for predicting global solar radiation in West Africa. *Beni-Suef University Journal of Basic and Applied Sciences*, *7*(4), 367-396.
Ododo, J. C., Sulaiman, A. T., Aidan, J., Yuguda, M. M., & Ogbu, F. A. (1995). The importance of maximum air temperature in the parameterisation of solar radiation in Nigeria. *Renewable Energy*, *6*(7), 751-763.
Ögelman, H., Ecevit, A., & Tasdemiroğlu, E. (1984). A new method for estimating solar radiation from bright sunshine data. *Solar energy*, *33*(6), 619-625.
Ogunbo, J. N., Alagbe, O. A., Oladapo, M. I., & Shin, C. (2020). N-hidden layer artificial neural network architecture computer code: geophysical application example. *Heliyon*, *6*(6), e04108
Ohunakin, O. S., Adaramola, M. S., Oyewola, O. M., & Fagbenle, R. O. (2013). Correlations for estimating solar radiation using sunshine hours and temperature measurement in Osogbo, Osun State, Nigeria. *Frontiers in Energy*, *7*(2), 214-222.
Ojosu, J. O., & Komolafe, L. K. (1987). Models for estimating solar radiation availability in South Western Nigeria. *Nigerian Journal of Solar Energy*, *16*(1987), 69-77.
Okundamiya, M. S., Emagbetere, J. O., & Ogujor, E. A. (2016). Evaluation of various global solar radiation models for Nigeria. *International Journal of Green Energy*, *13*(5), 505-512.
Olayinka, S. (2011). Estimation of global and diffuse solar radiations for se-lected cities in Nigeria. *International Journal of Energy and Environmental Engineering*, *2*(3), 13-33.
Olomiyesan, B. M., & Oyedum, O. D. (2016). Comparative study of ground measured, satellite-derived, and estimated global solar radiation data in Nigeria. *Journal of solar energy*, *2016*(1), 8197389.
Olubusade, J. E., Oyedum, O. D., Aibinu, A. M., & Ezenwora, J. A. (2022). Development of a model for ground measured and satellite-derived GSR data. *International Research Journal of Environmental Sciences*, *11*(3), 27-34.
Ouali, K., & Alkama, R. (2014). A new model of global solar radiation based on meteorological data in Bejaia City (Algeria). *Energy Procedia*, *50*, 670-676.
Page, J. K. (1961). IMe estimation of monthly mean values of daily total short wave radiation on-vertical and inclined surfaces from sun shine records for latitudes 400 N–400 S. In *Proceedings of the United Nations Conference on New Sources of Energy* (Vol. 98, No. 4, pp. 378-390).
Paltridge, G. W., & Proctor, D. (1976). Monthly mean solar radiation statistics for Australia. *Solar Energy*, *18*(3), 235-243.
Piedallu, C., & Gégout, J. C. (2007). Multiscale computation of solar radiation for predictive vegetation modelling. *Annals of Forest Science*, *64*(8), 899-909.
Prescott, J. A. (1940). Evaporation from a Water Surface in Relation to Solar Radiation. *Transactions of the Royal Society of South Australia, 64,* 114-118.
Quej, V. H., Almorox, J., Arnaldo, J. A., & Saito, L. (2017). ANFIS, SVM and ANN soft-computing techniques to estimate daily global solar radiation in a warm sub-humid environment. *Journal of Atmospheric and Solar-Terrestrial Physics*, *155*, 62-70.
Quej, V. H., Almorox, J., Ibrakhimov, M., & Saito, L. (2016). Empirical models for estimating daily global solar radiation in Yucatán Peninsula, Mexico. *Energy conversion and management*, *110*, 448-456.
Raja, I. A. (1994). Insolation-sunshine relation with site elevation and latitude. *Solar Energy*, *53*(1), 53-56.
Rensheng, C., Shihua, L., Ersi, K., Jianping, Y., & Xibin, J. (2006). Estimating daily global radiation using two types of revised models in China. *Energy Conversion and Management*, *47*(7-8), 865-878.
Rietveld, M. R. (1978). A new method for estimating the regression coefficients in the formula relating solar radiation to sunshine. *Agricultural Meteorology*, *19*(2-3), 243-252.
Sabbagh, J. A., Sayigh, A. A. M., & El-Salam, E. A. (1977). Estimation of the total solar radiation from meteorological data. *Solar energy*, *19*(3), 307-311.
Sánchez, G., Serrano, A., & Cancillo, M. L. (2012). Effect of cloudiness on solar global, solar diffuse and terrestrial downward radiation at Badajoz (Southwestern Spain). *Optica pura y aplicada*, *45*(1), 33-38.
Shahin, M. A., Jaksa, M. B., & Maier, H. R. (2008). State of the art of artificial neural networks in geotechnical engineering. *Electronic Journal of Geotechnical Engineering*, *8*(1), 1-26.
Sharkawy, A. N. (2024). T he effect of increasing hidden layers

on the performance of the deep neural network: Modelling, investigation, and evaluation. *Research on Engineering Structures and Materials*, *11*(4), 1633-1651.
Shen, B. W., Pielke Sr, R., Zeng, X., Cui, J., Faghih-Naini, S., Paxson, W., Kesarkar, A., Zeng, X., & Atlas, R. (2022). The dual nature of chaos and order in the atmosphere. *Atmosphere*, *13*(11), 1892.
Shepherd, G. M. (Ed.). (2003). *The synaptic organization of the brain.* Oxford University Press.
Skakun, A. A., & Volobuev, D. M. (2017). Contribution of the solar constant variations to calculations of insolation for the Holocene period. *Geomagnetism and Aeronomy*, *57*(7), 902-905.
Sonmete, M. H., Ertekin, C., Menges, H. O., Hacıseferoğullari, H., & Evrendilek, F. (2011). Assessing monthly average solar radiation models: a comparative case study in Turkey. *Environmental Monitoring and Assessment*, *175*(1), 251-277.
Swartman, R. K., & Ogunlade, O. (1967). Solar radiation estimates from common parameters. *Solar energy*, *11*(3-4), 170-172.
Teke, A., & Yıldırım, H. B. (2014). Estimating the monthly global solar radiation for Eastern Mediterranean Region. *Energy conversion and management*, *87*, 628-635.
Teke, A., Yıldırım, H. B., & Çelik, Ö. (2015). Evaluation and performance comparison of different models for the estimation of solar radiation. *Renewable and sustainable energy reviews*, *50*, 1097-1107.
Temmer, M. (2021). Space weather: The solar perspective: An update to Schwenn (2006). *Living Reviews in Solar Physics*, *18*, Article number 4.
Thornton, P. E., & Running, S. W. (1999). An improved algorithm for estimating incident daily solar radiation from measurements of temperature, humidity, and precipitation. *Agricultural and Forest Meteorology*, *93*(4), 211-228.
Torshizi, M. V., & Mighani, A. H. (2017). The application of solar energy in agricultural systems. *Journal of Renewable Energy and Sustainable Development*, *3*(2), 234-240.
Veeraboina, P., & Guduri, G. Y. (2014). Analysis of yearly solar radiation by using correlations based on ambient temperature: India. *Sustainable Cities and Society*, *11*, 16-21.
Walczak, S., & Cerpa, N. (1999). Heuristic principles for the design of artificial neural networks. *Information and Software Technology*, *41*(2), 107-117.
Wald, L. (2019). Basics in Solar Radiation at Earth Surface. *HAL Science Ouverte*, *1*(July).
Wallace, J. M., & Hobbs, P. V. (2006). *Atmospheric science: An introductory survey* (Vol. 92). Elsevier.
Weiss, A., Hays, C. J., Hu, Q., & Easterling, W. E. (2001). Incorporating bias error in calculating solar irradiance: implications for crop yield simulations. *Agronomy Journal*, *93*(6), 1321-1326.
Winslow, J. C., Hunt Jr, E. R., & Piper, S. C. (2001). A globally applicable model of daily solar irradiance estimated from air temperature and precipitation data. *Ecological Modelling*, *143*(3), 227-243.
Wu, G., Liu, Y., & Wang, T. (2007). Methods and strategy for modeling daily global solar radiation with measured meteorological data–A case study in Nanchang station, China. *Energy Conversion and Management*, *48*(9), 2447-2452.
Xu, C., Chen, S., Ren, H., Xu, C., Li, G., Li, T., & Sun, Y. (2025). A novel deep learning and GIS integrated method for accurate city-scale assessment of building facade solar energy potential. *Applied Energy*, *387*, 125600.
Xue, X., & Zhou, H. (2019). Soft computing methods for predicting daily global solar radiation. *Numerical Heat Transfer, Part B: Fundamentals*, *76*(1), 18-31.
Yadav, A. K., & Chandel, S. S. (2014). Solar radiation prediction using Artificial Neural Network techniques: A review. *Renewable and Sustainable Energy Reviews*, *33*, 772-781.
Yelmen, B., Çakır, M. T., & Ün, Ç. (2022). Estimation of Average Monthly Total Solar Radiation on a Horizontal Surface for the Central Anatolia Region: Example of Sivas Province. *Transactions of Famena*, *46*(2), 1-14.
Zabara, K. (1986). Estimation of the global solar radiation in Greece. *Solar & wind technology*, *3*(4), 267-272.